Research Article

Normidatul Salwa Sobri, Khisbullah Hudha, Zulkiffli Abd Kadir*, Noor Hafizah Amer, Ku Zarina Ku Ahmad and Mohd Sabirin Rahmat

Parameter optimization of anisotropic polarization in magnetorheological elastomers for enhanced impact absorption capability using the Taguchi method

https://doi.org/10.1515/jmbm-2024-0003 received August 22, 2023; accepted March 23, 2024

Abstract: Magnetorheological elastomers (MREs) are intelligent materials that exhibit changes in their properties when exposed to a magnetic field. By applying a magnetic field during the curing process, MRE can be made anisotropic. This study focuses on optimizing the fabrication process parameters using the design of an experimental approach, namely the Taguchi method. The parameters to be optimized for MRE fabrication include the number of coil turns, coil diameter, curing current, and curing time. Twenty-five sets of anisotropic MRE were fabricated and subjected to drop impact testing to evaluate their impact absorption capability. The results were further examined for a more comprehensive analysis using the signal-to-noise ratio, analysis of means, and analysis of variance. This rigorous examination aimed to pinpoint the optimal parameters and the key factors influencing the fabrication of the MRE. From the analysis result, it can be seen that the number of coil turns contributed to 63.36% of the entire MRE fabrication process. Furthermore, a well-defined composition for the MRE was identified, consisting of 200 coil turns, a coil diameter of 1.0 mm, an applied current of 1.2 A, and a curing time of 20 min.

Keywords: MRE, anisotropic polarization, Taguchi method

Normidatul Salwa Sobri, Khisbullah Hudha, Noor Hafizah Amer, Ku Zarina Ku Ahmad: Department of Mechanical Engineering, Universiti Pertahanan Nasional Malaysia, Sungai Besi Camp, 57000, Kuala Lumpur. Malaysia

Mohd Sabirin Rahmat: Department of Mechanical and Manufacturing, Faculty of Engineering and Built Environment, Universiti Kebangsaan Malaysia, 43600, Selangor, Malaysia

1 Introduction

Magnetorheological elastomers (MREs) are a class of smart materials that consist of an elastomer matrix containing ferrous particles. When subjected to a magnetic field, the ferrous particles within the MRE align themselves with the field's direction, resulting in an anisotropic MRE. This characteristic has the potential to enhance the properties and performance of MREs. Alam et al. [1] noted that the anisotropy of MRE depends on various factors, including the type of iron particle, the rubber matrix, the polymer-filler interface, the interactions between the polymer and filler, and the duration and strength of the applied magnetic field during the curing process (Figure 1). The application background of MRE encompasses various practical uses and contexts. These include applications in vibration and noise control, where MRE is utilized in dampers and isolators to mitigate vibrations and reduce noise levels in machinery [2–5]. In automotive applications, MRE is found to be used in suspension systems, engine mounts, and impact-absorbing components in vehicles [6-11]. The ability of MRE to rapidly adjust stiffness in response to changing conditions is particularly valuable, contributing to enhanced ride comfort and improved vehicle safety. Moreover, MRE extends its application to biomechanical devices, playing a role in prosthetics, orthopedic devices, and wearable technologies. In this context, MRE provides adjustable support and damping, leading to improved comfort and enhanced performance in various biomechanical applications. Additionally, MRE can serve as energy-harvesting devices, where mechanical vibrations or motions are converted into electrical energy through the variable properties of the material [12,13].

Different matrix materials have been employed in MRE production [14], including polyurethane, silicone rubber, natural rubber, and thermoplastic elastomers. Among them, silicone rubber is the most widely used matrix material [15].

^{*} Corresponding author: Zulkiffli Abd Kadir, Department of Mechanical Engineering, Universiti Pertahanan Nasional Malaysia, Sungai Besi Camp, 57000, Kuala Lumpur, Malaysia, e-mail: zulkiffli@upnm.edu.my

2 — Normidatul Salwa Sobri et al. DE GRUYTER

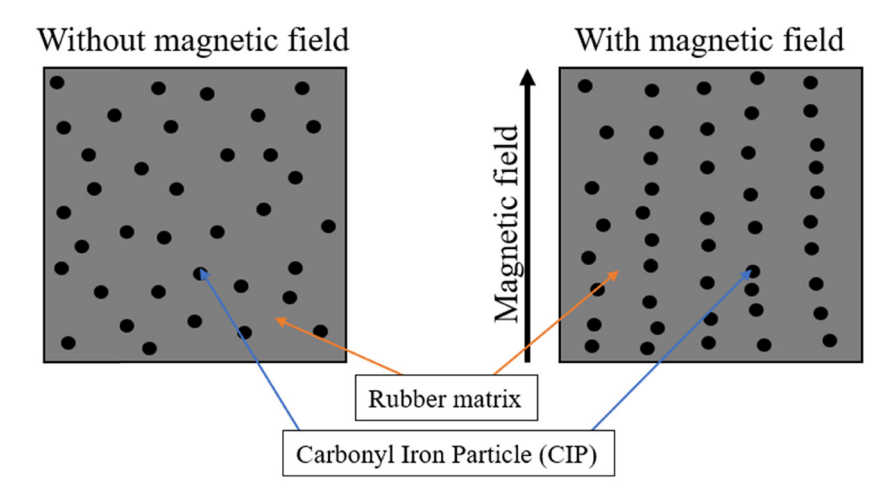


Figure 1: Schematic diagram of the general composition of MRE.

Micro-sized carbonyl iron particles, also known as CIPs, are the most commonly used fillers in MRE manufacturing due to their high magnetization at saturation [16]. The dispersion of iron particles throughout the material significantly affects the properties of MREs. During the cross-linking process, the application of an external magnetic field facilitates the formation of properly aligned chain-like structures [2]. Anisotropic MREs are characterized by particles arranged in a chain-like structure, while isotropic MREs have randomly distributed particles throughout the material. To initiate the polarization of the MRE and induce a magnetic field, specific parameters need to be initialized. This process requires essential equipment such as a coil and a power supply to ensure the successful completion of the curing process. Typically, MREs are exposed to a magnetic field generator during experimentation to reflect their sensitivity to magnetic forces [17]. Incorporating an external magnetic field generator in the experimental setup is crucial to accurately assess the MRE's response to magnetic forces during the curing process and subsequent testing of its elastic physical properties. The curing process aims to demonstrate the MRE's ability to exhibit different responses based on the strength of the magnetic force. To achieve this, two main components form the apparatus: an electromagnet and a high-precision DC excitation source. During the experiment, the magnetic field generator allows the researcher to adjust the external current and the size of the air gap, resulting in a magnetic field strength ranging from 600 to 700 mT. Additionally, Alam et al. [1] employed magnetic equipment to create anisotropic unvulcanized composites.

The design of experiment (DOE) is employed to aid in parameter selection and to determine the optimal parameters. DOE, which falls under the field of applied statistics, encompasses the planning, execution, analysis, and interpretation of controlled tests to evaluate factors that influence the value of a parameter or a group of parameters. It serves as a powerful tool for data collection and analysis in various experimental scenarios. By manipulating multiple input factors simultaneously, DOE allows for the assessment of their impact on the desired output or response. This approach enables the identification of significant interactions that may be overlooked when studying one factor at a time. Researchers can explore all possible combinations or choose a subset of combinations to investigate. Therefore, DOE optimizes the experimental conditions or processes themselves. There are several approaches to DOE, including factorial design, the Taguchi method, and response surface design. Factorial designs can be categorized into full factorial and 2^k factorial designs. Full factorial designs involve varying one factor at a time, conducting a large number of experiments, and capturing all interactions [18]. On the other hand, 2^k factorial designs are often used for preliminary experimentation only. The outcomes of a factorial experiment aid in determining the relative importance of each factor and provide insights into interaction effects. Another approach, the Taguchi method, was developed by Dr. Taguchi of Nippon Telephones and Telegraph Company [19]. This method relies on orthogonal array (OA) experiments, which provide a well-balanced set of minimum experiments serving as an objective function for optimization. Response surface methodology (RSM) is another approach within DOE that utilizes statistical, graphical, and mathematical techniques to develop, enhance, or optimize a process. It is particularly useful for variables influenced by multiple independent variables [20]. In this study, the Taguchi method was chosen to optimize the

parameters for anisotropic MRE polarization. The Taguchi method is effective in reducing output variance while allowing controlled input variations, thereby ensuring robustness in the process or product. It enables the controlled variation of parameters, such as a one-at-a-time approach.

Recently, several studies have emphasized the impact absorption capability (IAC) of MREs, e.g., Ledezma-Ramírez et al. [21] discuss the design and modeling of a variable stiffness impact damper using MREs, which are elastomers with embedded ferromagnetic particles. The proposed damper allows for controlled stiffness variations by the application of a magnetic field, aiming to enhance energy absorption and dissipation during impacts. Experimental quantification of prototypes reveals the damper's capacity to change stiffness, as well as its energy absorption and vibration suppression capabilities. Meanwhile, Poojary et al. [22] investigate the influence of the matrix material on the rheological properties of MREs by varying carbonyl iron particle content. Different rubber matrices (natural rubber, silicone rubber, and nitrile butadiene rubber) with varying particle concentrations are analyzed through forced transmissibility tests. Results show that the dynamic stiffness of MREs is highest for nitrile butadiene rubber and lowest for silicone rubber. The addition of carbonyl iron particles significantly improves stiffness, with the effect depending on the properties of the unfilled matrix. The findings underscore the importance of matrix type and filler concentration in determining the field-dependent response of MREs, which is crucial for optimizing their IACs. However, this study specifically tested the application of anisotropic MREs for impact mitigation. Consequently, precise values for the optimal parameters of anisotropic polarization were obtained, along with the determination of parameter dominancy percentages. The Taguchi method was employed in the experimental design to identify the optimum parameters and assess the dominancy percentage of each parameter. Furthermore, factorial design was utilized to improve the process of determining the optimal parameters for anisotropic polarization. Thus, the Taguchi method proves valuable in determining the optimal parameters for anisotropic MRE polarization.

The structure of this article is organized as follows: an introduction and previous works of MRE are presented in Section 1. In Section 2, the fabrication approach for MREs utilizing the Taguchi method is described along with the experimental methodology involving drop impact testing to assess IAC. A detailed analysis of the best polarization parameters and the dominant parameters is presented in Section 3. Finally, the findings obtained in this study are shown in Section 4.

2 Fabrication and experimental test of anisotropic MRE using the Taguchi method

The aim of this study is to optimize the IAC of an anisotropic MRE by identifying its parameters. As this is the initial study, no other quality characteristics, including potential side effects, will be considered. First, the chosen levels for the factors ensure that there will be no failures during the experiment that would require termination. The goal of the study is to maximize the IAC, using the Taguchi method by considering "the larger-the-better" approach as the objective function. The selection of the OA will be based on the chosen factors and levels.

2.1 Arrangement of MRE parameters using the Taguchi method

In this study, an OA with four factors and five levels is employed, resulting in the formation of the L²⁵ (5⁴) set of experiments [23]. These factors represent the parameters used in the curing process, namely the number of coil turns, the diameter of the coil, the current, and the curing time. Each factor has five levels, which are determined based on previous research findings. For instance, the number of coil turns ranges from 150 to 350 turns [24-26], the coil diameter varies from 0.4 to 1.6 mm, the current ranges from 0 to 2 A [27], and the curing time spans from 5 to 25 min [28,29]. Table 1 presents the L^{25} (5⁴) OA with four factors and five levels, while Table 2 outlines the selected factors and their respective levels.

The number of coil turns is selected within the range of 150-350, taking into account the diameter of the coil. These two parameters are interdependent and play a crucial role in determining their respective value ranges. Additionally, the current supplied by the power source is a key factor in generating the magnetic field required for the curing process. The maximum current applied for the lower coil diameter is 2.0 A. Consequently, this study utilizes a current range of 0.4-2.0 A. The curing time is limited to 25 min to prevent overheating of the coil. Therefore, a curing time range of 5-25 min is selected.

2.2 Fabrication of MRE based on L_{25} (5⁴)

To fabricate the anisotropic MREs, a total of 25 sets are produced using the generated OA from the L²⁵ (5⁴) table

Table 1: L₂₅ OA

Table 3: OA with the actual value of the parameters based on L_{25} (5^4)

Number of experiments	Number of turns	Diameter of the coil	Current	Time (min)	Number of experiments	Number of turns	Diameter of the coil	Current	Time (min)
1	1	1	1	1	1	150	0.4	0.4	5
2	1	2	2	2	2	150	0.7	0.8	10
3	1	3	3	3	3	150	1.0	1.2	15
4	1	4	4	4	4	150	1.3	1.6	20
5	1	5	5	5	5	150	1.6	2.0	25
6	2	1	2	3	6	200	0.4	0.8	15
7	2	2	3	4	7	200	0.7	1.2	20
8	2	3	4	5	8	200	1.0	1.6	25
9	2	4	5	1	9	200	1.3	2.0	5
10	2	5	1	2	10	200	1.6	0.4	10
11	3	1	3	5	11	250	0.4	1.2	25
12	3	2	4	1	12	250	0.7	1.6	5
13	3	3	5	2	13	250	1.0	2.0	10
14	3	4	1	3	14	250	1.3	0.4	15
15	3	5	2	4	15	250	1.6	0.8	20
16	4	1	4	2	16	300	0.4	1.6	10
17	4	2	5	3	17	300	0.7	2.0	15
18	4	3	1	4	18	300	1.0	0.4	20
19	4	4	2	5	19	300	1.3	0.8	25
20	4	5	3	1	20	300	1.6	1.2	5
21	5	1	5	4	21	350	0.4	2.0	20
22	5	2	1	5	22	350	0.7	0.4	25
23	5	3	2	1	23	350	1.0	0.8	5
24	5	4	3	2	24	350	1.3	1.2	10
25	5	5	4	3	25	350	1.6	1.6	15

Table 2: Factors and levels for anisotropic MRE curing setup parameters

Parameters	Level 1	Level 2	Level 3	Level 4	Level 5
Number of turns	150	200	250	300	350
Diameter of the	0.4	0.7	1.0	1.3	1.6
coil (mm)					
Current (A)	0.4	8.0	1.2	1.6	2.0
Time (min)	5	10	15	20	25

as a starting point. The specific values and levels for each parameter are listed in Table 3. Utilizing the information provided in Table 3, the anisotropic MREs are polarized to create the desired configuration. These fabricated MRE samples will be subjected to testing in order to identify the parameter combination that yields the highest IAC.

Table 3 presents the combinations of anisotropic MRE polarization parameters for each experiment. The manufacturing process of the anisotropic MRE involves subjecting it to a magnetic field during the curing process. The ratio of room-temperature-vulcanizing (RTV) silicone rubber to carbonyl iron powder (CIP) is 40:60, as reported by Burhannuddin *et al.* [30]. The hardener is added to the RTV

silicone rubber, with a weight proportion of 3% relative to the RTV silicone rubber. The fabrication process of the anisotropic MRE is shown in Figure 2, and Table 4 shows the detailed breakdown of the weight of materials used in the fabrication of the anisotropic MRE.

As shown in Figure 2, a weighing scale is used to measure the quantities of RTV silicone rubber, CIP, and hardener. The proportions of these materials utilized in the MRE fabrication are outlined in Table 4. The fabrication process of the MRE involves several stages, namely mixing, pouring, and curing. Initially, the RTV silicone rubber and CIP are manually mixed in a measuring cup, and then the hardener is added to the mixture. Subsequently, the prepared mixture is poured into a mold that has been treated with a mold release agent. Following the pouring stage, the MRE undergoes curing in the presence of a magnetic field. The setup for the curing process is illustrated in Figure 3.

As illustrated in Figure 3, the selection of factors is crucial for the setup of the curing process, which involves the use of coils to generate a magnetic field. Therefore, the diameter and number of turns of the coil are important factors to consider. Additionally, the power supply that generates the current for the magnetic field plays a

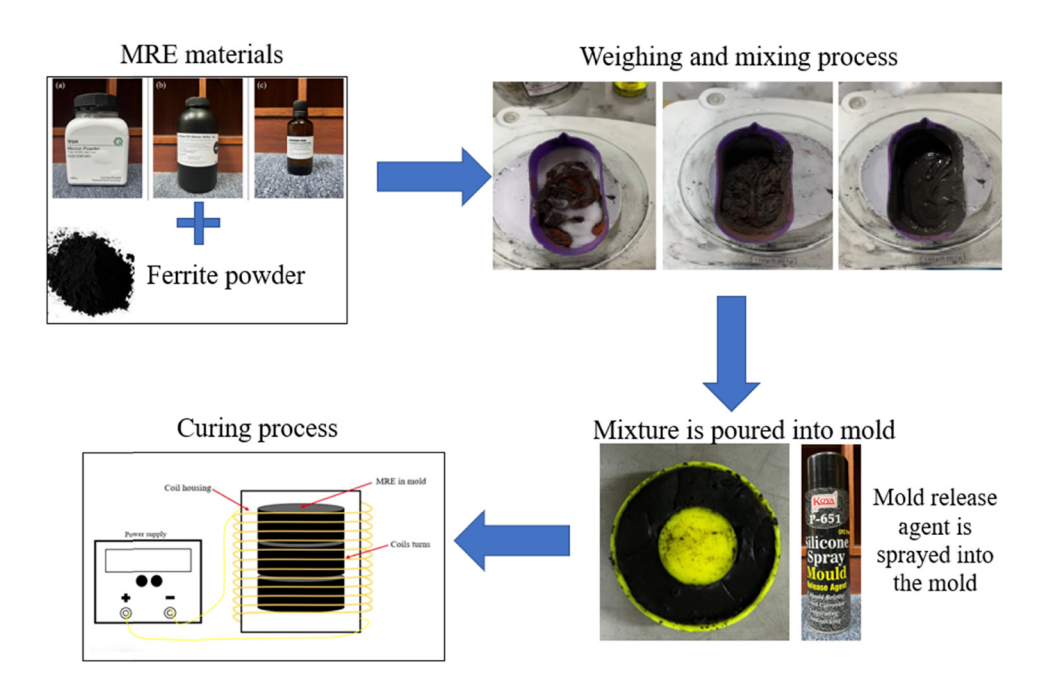


Figure 2: Fabrication process of the anisotropic MRE.

Table 4: Weight of the materials for anisotropic MRE fabrication

Material	Percentage	Weight (g)
RTV silicone rubber	40%	12
Carbonyl iron powder	60%	18
Hardener	3% of the RTV SR	0.36

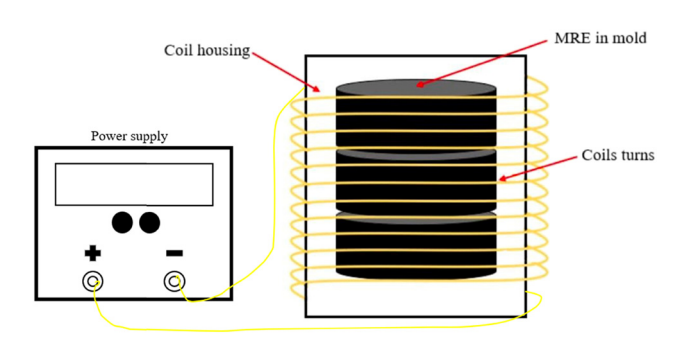


Figure 3: Curing process setup of anisotropic MRE.

significant role. Consequently, variations in the current are essential for generating the required magnetic field during the curing process. Finally, it is essential to expose the MRE to the magnetic field for at least the same duration as the curing time, or longer, to ensure proper curing. This is the stage in the curing process where the parameters from the OA come into play. For example, the first set consists of all the factors at the first level, indicating that the coil has 150 turns with a diameter of 0.4 mm. The current configuration

will be 0.4 A, and the curing time will be 5 min. The drop impact test will be conducted on each of the 25 MRE sets, which comprise different combinations of successfully fabricated parameters and levels.

2.3 Drop impact testing

In this study, the IAC of the MREs was evaluated through a drop impact test conducted in accordance with ASTM D2444 and ISO 3127 standards. The purpose of this test is to assess the material's ability to withstand sudden external forces. The drop impact test is commonly used to determine the impact resistance of various materials, including thermoplastic pipes. For this experiment, an Instron Drop Impact Machine and CEAST Software were utilized to control the test parameters, including impact energy, impact velocity, falling height, tup holder mass, tup nominal mass, specimen support, and applied current. The specifications for these parameters are provided in Table 5.

Figures 4 and 5 show the experimental setup and the setup for the drop impact test, respectively. As shown in Figure 4, the MRE is positioned between two metal plates to prevent its breakage and compression. During the experiment, the impact is applied to the impactor. To induce shear movement during impact, a sleeve angle of 30° was deliberately chosen. The coil bobbin, composed of the Teflon material, accommodates a copper enamel wire with a diameter of 0.7 mm, which is wound around it.

Table 5: Parameters of the impact test

Parameter	Value
Impact energy	11 J
Impact velocity	2.00 m/s
Falling height	204 mm
Tup holder mass	4.3 kg
Tup nominal mass	1.2 kg
Specimen support	3 mm
Current	0.0, 0.5, 1.0, 1.5, 2.0 A

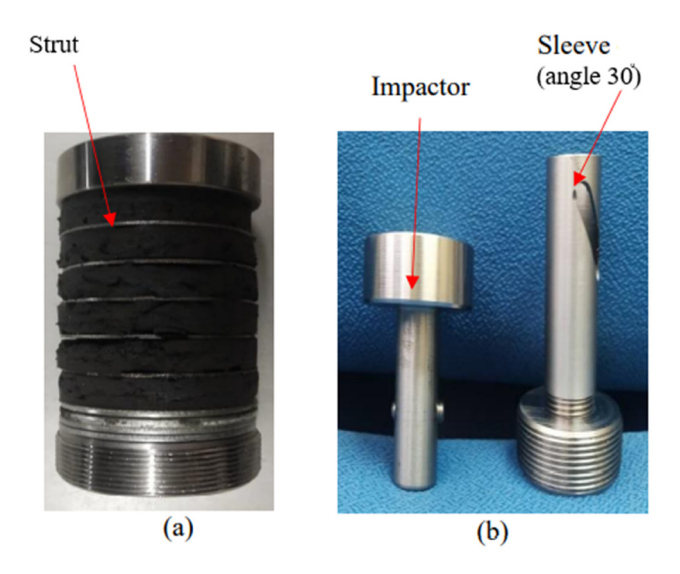


Figure 4: The MRE test device.

As shown in Figure 4(a), the MRE specimen is contained within a specialized MRE device designed for testing its properties. Meanwhile, in Figure 4(b), the MRE strut is inserted alongside the impactor and the sleeve, which are inclined at a 30° angle. This entire device is then placed inside the specimen space of the drop impact test machine, as shown in Figure 5.

Figure 5 shows a hydraulic system that pulls the impact weight to the release position before initiating the release. The impact weight is equipped with an accelerometer and load cell to capture real-time acceleration and impact force data. This test is crucial for evaluating the material's behavior under impact loading conditions. The initial step of the experiment involves confirming the parameters for the drop impact loading. The desired falling height for the impactor is set, and it is dropped onto the specimen within a time frame of 3 s. Throughout the impact, sensors record data, which are subsequently transmitted to the data acquisition (DAQ) system. The obtained raw data include time, displacement, and force measurements.

2.4 Calculation of the IAC

The IAC of the MRE is calculated using the force—displacement characteristics obtained from the experiment. Figure 6 presents a typical force—displacement (*F*–*d*) characteristic curve for the MRE. In this graph, the blue line represents



Figure 5: The setup for the drop impact test.

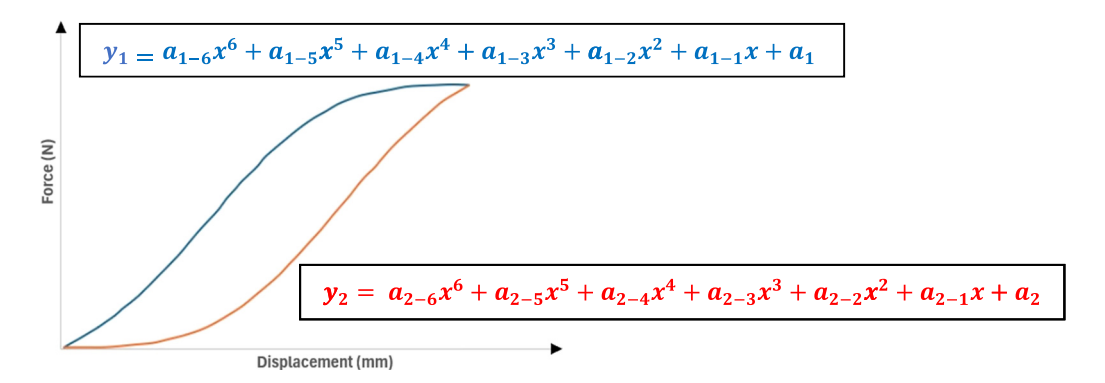


Figure 6: *F–d* characteristic graph of MRE with functions.

the compression state of the MRE, where the force increases progressively with displacement during the impact. On the other hand, the red line indicates the extension state of the MRE, where the force decreases as the displacement returns to its original state. The IAC is estimated by calculating the area under the *F*–*d* curve. To determine the area under the curve or the IAC, polynomial functions are generated based on the blue and red lines. However, it is important to note that polynomial models based on only a few data points may not be ideal for making accurate predictions, as there are numerous polynomial functions that can fit a given set of data points. Figure 6 provides an illustration of a typical *F*–*d* graph with associated polynomial functions.

Based on Figure 6, polynomial functions of the sixth order are generated from the F-d graph to represent the ascending line (y_1) and descending line (y_2) . These functions can be expressed by Eqs. (1) and (2):

$$y_1 = a_{1-6}x^6 + a_{1-5}x^5 + a_{1-4}x^4 + a_{1-3}x^3 + a_{1-2}x^2 + a_{1-1}x + a_1.$$
 (1)

$$y_2 = a_{2-6}x^6 + a_{2-5}x^5 + a_{2-4}x^4 + a_{2-3}x^3 + a_{2-2}x^2 + a_{2-1}x$$

$$+ a_2$$
(2)

In these equations, a_{i-j} is a real number, and x_{i-j} represents the displacement. The values of the constants depend on the shape of the curve. To determine the area under the F-d graph, the generated functions are then integrated. The formula for calculating the IAC is expressed by Eq. (3):

IAC =
$$\int_{x_{min}}^{x_{max}} (y_1 - y_2) dx$$
, (3)

where x_{max} represents the maximum displacement in the F-d graph, and x_{min} represents the initial displacement. In theory, as the absorption force increases, the displacement decreases, resulting in a wider shape of the F-d graph. The calculation of IAC is crucial for identifying the optimal composition of MRE for applications involving impact mitigation. Higher absorption capability during impact loading indicates better characteristics of MRE for such applications.

2.5 Experimental results of MRE drop impact test based on L_{25} (5⁴)

The test results of the drop impact test in terms of force and displacement serve as important characteristics. The IAC can be determined by extracting the values of y_1 and y_2 from the F-d graph, as explained in the previous section, and then calculated using Eq. (3). The obtained IAC values from the experiment are presented in Table 6. Table 6 shows the IAC values for different experiments, with experiment 7 exhibiting the highest IAC among those listed.

As shown in Table 6, experiment 7 demonstrates the highest IAC value of 10.23 N m with the greatest force of 15146.20 N and the highest displacement of 1.23 mm. Meanwhile, experiments 4 and 16 exhibit the lowest IAC values of 1.17 N m, with the maximum forces of 13994.61 and 17944.12 N, and maximum displacements of 1.13 and 0.31 mm, respectively. Once the 25 IAC values have been obtained, the subsequent process involves determining the significance and contribution of individual factors. This process will be sequentially executed through the following steps, involving the calculation of the signal-to-noise ratio (SNR), the analysis of means (ANOM), and the analysis of variance (ANOVA).

3 Optimization of anisotropic MRE

During the optimization process, the performance of the system was evaluated by analyzing the IAC obtained from the experimental tests. To ensure that the anisotropic MRE

Table 6: Experimental results and IAC values of each set

Number of experiments	Max. force (N)	Max. disp. (mm)	IAC (N m)
1	10437.88	1.54	2.22
2	14509.40	1.45	3.32
3	15316.69	1.17	1.58
4	13994.61	1.13	1.17
5	16003.63	1.24	2.45
6	15452.07	1.04	1.53
7	15146.20	1.23	10.23
8	15169.60	1.10	8.44
9	17979.22	1.06	7.15
10	16767.46	0.54	1.80
11	16623.72	0.32	1.41
12	17731.86	0.31	1.68
13	13677.05	0.14	1.19
14	17730.18	0.37	1.93
15	17817.10	0.34	1.85
16	17944.12	0.31	1.17
17	17146.87	0.34	1.44
18	18077.83	2.06	6.15
19	16349.61	0.27	1.24
20	16570.23	1.97	2.49
21	18522.43	2.12	6.78
22	17593.13	1.75	2.27
23	16058.79	2.16	4.67
24	15104.42	2.04	5.47
25	18527.44	1.91	4.23

meets the design specifications and minimizes errors, a performance indicator called the SNR is utilized. In order to meet the design requirements, SNR with a larger-the-better characteristic is preferred. The formula for SNR is as follows, where a larger value is considered more favorable:

SNR =
$$-10 \log \left(\frac{1}{n} \sum_{i=0}^{n} \frac{1}{IAC_i} \right)$$
 (4)

From Eq. (4), the variable n represents the number of repetitions. In this particular study, the number of repetitions is set to 1. The SNR value is calculated for each set of experiments, and the calculated values for all sets are presented in Table 7. To identify the combination of parameters that yields the most favorable results, it is crucial to calculate the total SNR value for each factor and its corresponding level. This can be achieved by employing the $L_{25}(5^4)$ OA, as illustrated in Table 1. This approach facilitates the evaluation of the optimal parameter combination with the highest potential for desirable outcomes.

The SNR values provided in Table 7 serve as the basis for calculating the total SNR values for each level, utilizing the information from Table 1. For example, to determine the total number of experiments for the curing time at level 2, experiments 2, 10, 13, 16, and 24 are considered. The corresponding SNR values obtained from Table 7 for these experiments are 10.42, 5.09, 1.51, 1.39, and 14.76, respectively. Consequently, the sum of the SNR values for the curing time at level 2 is recorded as 33.17. By following the same procedure for all available combinations, the total SNR values for each level can be calculated. The results of these calculations are presented in Table 8. Furthermore, Figure 7 shows the SNR ratio values for the various curing process parameters.

Based on the procedure outlined by the Taguchi method, the values obtained are plotted against the five levels in Figure 7. Through this analysis, it has been determined that the maximum SNR values for optimal characteristics occur at level 2 for the number of coil turns (68.02), level 3 for the diameter of the coil (54.98), level 3 for the current (51.41), and level 4 for the curing time (60.87). These findings indicate that the optimum parameters for polarization of the anisotropic MRE are summarized in Table 9.

After identifying the optimal parameters in Table 9, the next step of this study is to determine the overall most influential parameters. This is achieved by calculating ANOM using the previously determined SNR values. The ANOM for SNR can be calculated as follows:

$$ANOM = \frac{1}{X_0} \sum_{i=1}^{n} SNR_i.$$
 (5)

Based on Eq. (5), the number of levels is represented by x_0 , while the number of factors is denoted by i. For this particular analysis, $x_0 = 5$ and i = 1. The results of the ANOM for each parameter and level are given in Table 10.

Following the ANOM, the obtained ANOM values for each factor and level are utilized in ANOVA to explore the impact of different parameters on the overall performance of the curing setup. ANOVA is a widely used statistical method for assessing the relative importance of various variables and parameters in relation to the overall system performance. In this study, ANOVA is determined by calculating the sum of squares (SS) for each parameter. The SS can be computed using the following formula:

SS =
$$x \sum_{i=1}^{n} (m_i - m_{\text{avg}})^2$$
, (6)

where m_i is the ANOM value and the $m_{\rm avg}$ is the average value of the SNR. By evaluating the SS, the contribution of each parameter can be determined. The parameter with the highest contribution signifies its dominant influence or importance on the polarization of the anisotropic MRE. The percentage value of the contribution for each parameter is presented in Table 11.

Table 7: Calculation of SNR for every set of anisotropic MRE

Number of experiments	Number of turns	Diameter of the coil	Current	Time (min)	IAC	SNR
1	150	0.4	0.4	5	2.22	6.92
2	150	0.7	0.8	10	3.32	10.42
3	150	1	1.2	15	1.58	3.95
4	150	1.3	1.6	20	1.17	1.38
5	150	1.6	2	25	2.45	7.77
6	200	0.4	0.8	15	1.53	3.70
7	200	0.7	1.2	20	10.23	20.19
8	200	1	1.6	25	8.44	18.52
9	200	1.3	2	5	7.15	17.08
10	200	1.6	0.4	10	1.80	5.09
11	250	0.4	1.2	25	1.41	2.99
12	250	0.7	1.6	5	1.68	4.52
13	250	1	2	10	1.19	1.51
14	250	1.3	0.4	15	1.93	5.70
15	250	1.6	0.8	20	1.85	5.32
16	300	0.4	1.6	10	1.17	1.39
17	300	0.7	2	15	1.44	3.17
18	300	1	0.4	20	6.15	15.77
19	300	1.3	0.8	25	1.24	1.84
20	300	1.6	1.2	5	2.49	7.93
21	350	0.4	2	20	6.78	16.62
22	350	0.7	0.4	25	2.27	7.11
23	350	1	0.8	5	4.67	13.38
24	350	1.3	1.2	10	5.47	14.76
25	350	1.6	1.6	15	4.23	12.53

Table 8: Summation of SNR values

Parameters	Level 1	Level 2	Level 3	Level 4	Level 5	Total
Coil turns	30.43	64.59	20.06	30.10	64.41	209.60
Diameter	31.64	45.41	53.13	40.77	38.64	209.60
Current	40.60	34.67	49.84	38.35	46.15	209.60
Time	49.84	33.17	29.05	59.29	38.24	209.60

Table 11 provides an overview of the contributions made by the parameters to the enhancement of the performance of MRE. It is evident that the number of coil turns significantly influences the properties of MRE, accounting for 63.36% of the overall control parameters, followed by the curing time (22.2%), the diameter of the coil (9.15%), and the applied current (5.29%). By observing the impact of changing each parameter in the curing setup, it is evident that the number of coil turns has a greater influence on controlling the overall setup compared to the other parameters.

Based on the findings of the optimization process, the highest contribution of anisotropic MRE is the number of coil turns. The number of coils in the anisotropic MRE process is a critical factor that significantly influences the IAC in terms of its performance and functionality. Coils

play a crucial role in generating the magnetic field within the MRE, which affects its rheological properties and directly influences the strength of the magnetic field generated within the MRE. A higher number of coils generally results in a stronger magnetic field, enhancing the material's responsiveness to changes in the applied magnetic field. This responsiveness is essential for rapidly adjusting the MRE's mechanical properties during impact tests. Additionally, the optimized number of coils ensures a uniform distribution of the magnetic field across the MRE. This uniformity is important for achieving consistent IAC throughout the material, preventing localized stress concentrations, and enhancing overall performance. The second most significant contribution is attributed to the curing time in the MRE manufacturing process. The curing time directly 10 — Normidatul Salwa Sobri et al. DE GRUYTER

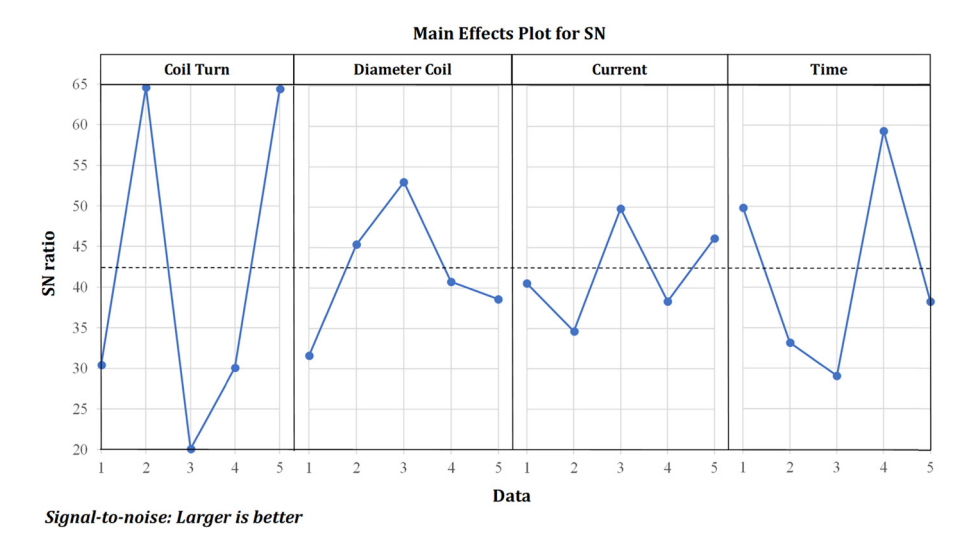


Figure 7: SNR for parameters of the curing setup.

Table 9: Optimum parameters for anisotropic MRE polarization

Parameters	Optimum value	Level
Number of coil turns	200 turns	2
Diameter of the coil	1.0 mm	3
Current	1.2 A	3
Curing time	20 min	4

Table 10: ANOM results for each parameter and levels

Parameters	Level 1	Level 2	Level 3	Level 4	Level 5	Total
Coil turns	6.09	12.92	4.01	6.02	12.88	41.92
Diameter	6.33	9.08	10.63	8.15	7.73	41.92
Current	8.12	6.93	9.97	7.67	9.23	41.92
Time	9.97	6.63	5.81	11.86	7.65	41.92

Table 11: Contributions of the parameters in the curing setup

Parameters	SS	Contribution of the parameter (%)
<u> </u>	252.04	62.26
Coil turns	353.94	63.36
Diameter	51.09	9.15
Current	29.54	5.29
Curing time	124.02	22.20
Total	558.59	100

affects the development of the MRE's internal structure and cross-linking between polymer chains. Adequate curing

time is essential for achieving optimal material integrity and strength. A well-cured MRE is better equipped to withstand and absorb impact forces, reducing the risk of material failure during high-stress tests.

4 Conclusions

In this study, anisotropic MRE was fabricated by carefully selecting the curing process parameters. The goal was to optimize the anisotropic MRE by improving its IAC. To achieve this, the Taguchi method was employed to determine the optimal parameters for anisotropic polarization. The investigation commenced by identifying the OA, considering the selected factors and parameter levels. The L₂₅ (5⁴) OA combination was utilized to fabricate the anisotropic MRE. Subsequently, the drop impact test was performed on all 25 sets of anisotropic MREs. The results obtained were subjected to analysis using several techniques, including IAC, Taguchi analysis, SNR, ANOM, and ANOVA. The analysis revealed the significant contributions of the parameters: the number of coil turns accounted for 63.36% of the IAC improvement, followed by the curing time (22.2%), the diameter of the coil (9.15%), and the current (5.29%). Based on the analysis, the optimal parameters for anisotropic MREs were identified as follows: 200 coil turns (Level 2), 1.0 mm coil diameter (Level 3), 1.2 A (Level 3) current, along with a curing time of 20 min (Level 4). This combination was substantiated through experimental testing, where it was demonstrated that the MRE yielded the highest IAC value in experiment 7.

5 Recommendations for future work

After successfully identifying the optimum parameters for the anisotropic MRE and demonstrating its ability to produce the highest IAC, this MRE can be applied as an active bumper system to mitigate frontal collisions in vehicles. The ongoing research project focuses on implementing this active bumper system to enhance vehicle safety. Frontal collisions are frequently deemed hazardous accidents because of their direct impact on the vehicle body and occupants. By integrating the MRE actuator between the passive bumper system and the front vehicle body, namely the crumple zone, the impact energy can be effectively minimized. This could help to protect the vehicle structure from damage and minimize the risk of injury to occupants.

Funding information: This research is fully supported by FRGS grant, FRGS/1/2021/TK02/UPNM/02/1 led by K. Hudha. The authors acknowledge the Ministry of Higher Education (MOHE) and the National Defence University of Malaysia for the approved funding, which made this important research viable and effective.

Author contributions: Normidatul Salwa Sobri: fabrication and experimental tests. Khisbullah Hudha: basic study design, interpretation of results, and data collection. Zulkiffli Abd Kadir: manuscript writing, optimization method, interpretation of results, and data collection. Noor Hafizah Amer: dynamic analysis. Ku Zarina Ku Ahmad: analysis of mechanical properties. Mohd Sabirin Rahmat: material fabrication.

Conflict of interest: The authors declare no conflict of interest.

Data availability statement: Data sharing is not applicable to this article as no datasets were generated or analysed during the current study.

References

- Alam MN, Kumar V, Ryu SR, Choi J, Lee DJ. Anisotropic magnetor-[1] heological elastomers with carbonyl iron particles in natural rubber and acrylonitrile butadiene rubber: A comparative study. J Intell Mater Syst Struct. 2021;32(14):1604-13.
- Lee CJ, Kwon SH, Choi HJ, Chung KH, Jung JH. Enhanced magnetorheological performance of carbonyl iron/natural rubber composite elastomer with gamma-ferrite additive. Colloid Polym Sci. 2018;296(9):1609-13.
- Xu L, Zou A, Fu J, Yu M, Bai J. Development and simulation evaluation of a magnetorheological elastomer isolator for

- transformer vibration control. Proceedings of the 30th Chinese Control and Decision Conference, CCDC 2018; 2018. p. 2600-4.
- [4] Jalali A, Dianati H, Norouzi M, Vatandoost H, Ghatee M. A novel bidirectional shear mode magnetorheological elastomer vibration isolator. J Intell Mater Syst Struct. 2020;31(17):2002-19.
- Sun S, Yang J, Yildirim T, Ning D, Zhu X, Du H, et al. A magnetor-[5] heological elastomer rail damper for wideband attenuation of rail noise and vibration. | Intell Mater Syst Struct. 2020;31(2):220-8.
- Bai XX, Deng XC, Shen S. Controllability of magnetorheological shock absorber: II. Testing and analysis. Smart Mater Struct. 2019;28(1).
- [7] Wang M, Chen Z, Wereley NM. Adaptive magnetorheological energy absorber control method for drop-induced shock mitigation. | Intell Mater Syst Struct. 2021;32(4):449-61.
- [8] Nguyen XB, Komatsuzaki T, Truong HT. Novel semiactive suspension using a magnetorheological elastomer (MRE)-based absorber and adaptive neural network controller for systems with input constraints. Mech Sci. 2020;11(2):465-79.
- [9] Kumar M, Kumar A, Bharti RK, Yadav HNS, Das M. A review on rheological properties of magnetorheological fluid for engineering components polishing. Mater Today: Proc. 2022;56:A6-A12.
- Mat Song R, Mazlan SA, Johari N, Imaduddin F, Abdul Aziz SA, Abd Fatah AY, et al. Semi-active controllable stiffness engine mount utilizing natural rubber-based magnetorheological elastomers. Front Mater. 2022;9:875787.
- [11] Gao P, Li H, Liu H, Xiang C. An innovative torsional vibration absorber of vehicle powertrain system: Prototype design, performance test, and control experiment. Mech Based Des Struct Mach. 2023;51(6):3434-66.
- [12] Brancati R, Rocca E, Russo R. Gear rattle reduction in an automotive driveline by the adoption of a flywheel with an innovative torsional vibration damper. Proc Inst Mech Eng Part K: | Multi-Body Dyn. 2019:233(4):777-91.
- [13] Zhu Z, Wang Z, Dai K, Wang X, Zhang H, Zhang W. An adaptive and space-energy efficiency vibration absorber system using a selfsensing and tunable magnetorheological elastomer. Nano Energy.
- [14] Kang SS, Choi K, Nam JD, Choi HJ. Magnetorheological elastomers: Fabrication, characteristics, and applications. Materials. 2020:13(20):1-24.
- [15] Bastola AK, Hossain M. A review on magneto-mechanical characterizations of magnetorheological elastomers. Compos Part B: Eng. 2020;200(May):108348.
- [16] Hapipi N, Aziz SAA, Mazlan SA, Ubaidillah, Choi SB, Mohamad N, et al. The field-dependent rheological properties of plate-like carbonyl iron particle-based magnetorheological elastomers. Results Phys. 2019;12(Dec 2018):2146-54.
- Li T, El-Aty AA, Cheng C, Shen Y, Wu C, Yang Q, et al. Investigate the effect of the magnetic field on the mechanical properties of silicone rubber-based anisotropic magnetorheological elastomer during curing process. J Renew Mater. 2020;8(11):1411-27.
- Siang JKK, Chia PZ, Koronis G, Silva A. Exploring the use of a full [18] factorial design of experiment to study design briefs for creative ideation. Proc ASME Des Eng Tech Conf. 2018;7:1-12.
- Freddi A, Salmon M. Introduction to the Taguchi method. Springer Tracts in Mechanical Engineering. Switzerland: Springer, Cham: 2019. p. 159-80.
- [20] Chelladurai SJS, Murugan K, Ray AP, Upadhyaya M, Narasimharaj V, Gnanasekaran S. Optimization of process parameters using

- response surface methodology: A review. Mater Today: Proc. 2020;37(Part 2):1301–4.
- [21] Ledezma-Ramírez DF, Rustighi E, Tapia-González PE. Design of a variable stiffness impact damper using magnetorheological elastomers. In Society for Experimental Mechanics Annual Conference and Exposition. Cham: Springer Nature Switzerland; 2023. p. 87–90.
- [22] Poojary UR, Kiran K, Hegde S, Gangadharan KV. An experimental investigation on the matrix dependent rheological properties of MRE. | Intell Mater Syst Struct. 2024;35(1):81–98.
- [23] Essa WK, Yasin SA, Abdullah AH, Thalji MR, Saeed IA, Assiri MA, et al. Taguchi L25 (5⁴) approach for methylene blue removal by polyethylene terephthalate nanofiber-multi-walled carbon nanotube composite. Water. 2022;14(8):1242.
- [24] Brancati R, Di Massa G, Genovese A. Experimental investigation to enhance performances of MRE in energy harvesting. In International Workshop IFToMM for Sustainable Development Goals. Cham: Springer Nature Switzerland; 2023. p. 3–10.
- [25] Li Y, Li J, Li W, Du H. A state-of-the-art review on magnetorheological elastomer devices. Smart Mater Struct. 2014;23(12):123001.

- [26] Rahmat MS, Hudha K, Kadir ZA, Nuri NRM, Amer NH, Abdullah S. Modelling and control of a Magnetorheological elastomer for impact reduction. J Mech Eng Sci. 2019;13(3):5259–77.
- [27] Hapipi N, Mazlan SA, Aziz SAA, Ubaidillah U, Choi S-B. Effect of curing current on stiffness and damping properties of magnetorheological elastomers. Int J Sustain Transp Technol. 2018:1(2):51–8.
- [28] Hafeez MA, Usman M, Umer MA, Hanif A. Recent progress in isotropic magnetorheological elastomers and their properties: A review. Polymers. 2020;12(12):1–35.
- [29] Lai NT, Ismail H, Abdullah MK, Shuib RK. Optimization of prestructuring parameters in fabrication of magnetorheological elastomer. Arch Civ Mech Enq. 2019;19(2):557–68.
- [30] Burhannuddin NL, Nordin NA, Mazlan SA, Aziz SAA, Kuwano N, Jamari SKM, et al. Physicochemical characterization and rheological properties of magnetic elastomers containing different shapes of corroded carbonyl iron particles. Sci Rep. 2021;11(1):1–17.